Available online at www.sciencedirect.com

SciVerse ScienceDirect

Ceramics International 39 (2013) 5379–5385

CERAMICS INTERNATIONAL

www.elsevier.com/locate/ceramint

Synthesis of Na_2FePO_4F/C and its electrochemical performance

Jingjing Zhou[a,b], Jiefeng Zhou[c], Yuanhao Tang[a], Yujing Bi[a], Chenyun Wang[a], Deyu Wang[a,*], Siqi Shi[b,**]

[a]*Ningbo Institute of Material Technology and Engineering, Chinese Academy of Sciences, Ningbo 315201, China*
[b]*Department of Physics, Center for Optoelectronics Materials and Devices, Zhejiang Sci-Tech University, Hangzhou 310018, China*
[c]*Zhejiang Tenglong Industry Group Co., Ltd., Ningbo 315040, China*

Received 24 October 2012; received in revised form 11 December 2012; accepted 12 December 2012
Available online 22 December 2012

Abstract

Using NaF as the only Na precursor, fluorophosphate Na_2FePO_4F/C materials have been synthesized via the solid-state reaction. Na_2FePO_4F starts to form at 300 °C, becomes the sole crystalline form between 400 and 600 °C, and decomposes at 650 °C. Comparing with the theoretical capacity of 124 mAh g^{-1}, the sample prepared at 600 °C delivered a discharge capacity of 118 mAh g^{-1}. The outstanding electrochemical performance is believed to result from the good crystallization and high purity of the synthesized materials. The capacity retentions at 0.5 C and 2 C are 95.8% and 89.8%, respectively, of that at 0.05 C. Furthermore, a discharge capacity of 122 mAh g^{-1} is maintained under the cycling between 2.0 and 5.2 V vs. Li/Li^+, indicating that the second Na^+ is not extracted from the Na_2FePO_4F lattice.

Keywords: Na_2FePO_4F; Mechanism of the solid-state reaction; NaF

1. Introduction

Recently, A_2MPO_4F materials (A = Li, Na; and M = Fe, Co, Mn) have attracted increasing research interests [1–7] due to the possibility to utilize two alkaline cations and the similar cyclic stability to olivine phosphates. In contrast to its Mn and Co containing counterparts [2,5], A_2FePO_4F is more attractive due to its good kinetic behavior and appropriate working potential [3,8]. Not only does Na_2FePO_4F has potential applications in lithium ion battery, but Na_2FePO_4F is also a good host to reversibly accommodate Na^+ ions [1,5]. These characteristics enable this series of materials to work as the Na ion battery cathode, which is considered as one of the most cost-effective technologies to stabilize the power output in new energy power plants [5,6].

In 2007, Ellis et al. [1] first proposed A_2FePO_4F compound. They synthesized Na_2FePO_4F via the solid-state reaction, and then obtained $LiNaFePO_4F$ and Li_2FePO_4F via the chemical ion-exchange reaction. Their results indicated a possibility to use Na_2FePO_4F as the high-capacity cathode material since both Na^+ ions were chemically removable. In the subsequent studies [6,7,9], the solid-state reaction was also widely used to prepare this material. However, the optimum preparation methods and inherent reaction mechanisms still need further investigation.

Generally, mixed Na salts such as NaF and $NaHCO_3$ (1:1 in mole) were used as the Na precursors for synthesizing Na_2FePO_4F via the solid-state reaction. However, Na_3PO_4 impurity was detected in the sample synthesized via the above mixed Na salts in our previous experiments. Similarly, Li_3PO_4 was easily formed when Li_2CO_3 was utilized to prepare $LiFePO_4$ [10]. Our previous work has proved that LiF was a better lithium source than Li_2CO_3

---

*Corresponding author. Tel./fax: +86 574 8668 8084.
**Corresponding author. Tel./fax: +86 571 8684 3655.
E-mail addresses: wangdy@nimte.ac.cn (D. Wang), siqishihz@gmail.com (S. Shi).

0272-8842/$ - see front matter © 2012 Elsevier Ltd and Techna Group S.r.l. All rights reserved.
http://dx.doi.org/10.1016/j.ceramint.2012.12.044

to prepare olivine phosphates since its medium activity suppressed the Li_3PO_4 formation [10]. Furthermore, Li–F bond could be broken at ~400 °C and F element was released in the form of HF gas when synthesizing $LiFePO_4$ [10] and $Li_3V_2(PO_4)_3$ [11]. Based on the above considerations, it could be a convenient route to synthesize Na_2FePO_4F materials with NaF alone.

In this paper, Na_2FePO_4F has been synthesized with NaF as the only Na precursor, and the reaction mechanisms are proposed for the first time. Pure phase of Na_2FePO_4F could be obtained at temperature between 400 and 600 °C. The sample obtained at 600 °C delivered the highest discharge capacity, best rate capability and excellent cyclic stability under the cycling between 2.0 and 4.5 V vs. Li/Li^+. Moreover, we explored the possibility of utilizing the second Na^+ in Na_2FePO_4F/C by cycling between 2.0 and 5.2 V vs. Li/Li^+.

2. Experimental

The carbon-coated Na_2FePO_4F/C was prepared via the solid-state reaction using NaF as the only Na precursor. A stoichiometric amount of NaF (Aladdin, AR), $FeC_2O_4 \cdot 2H_2O$ (Alfa Aesar, AR) and $NH_4H_2PO_4$ (Aladdin, AR) was ground and mixed by ball-milling for 6 h with 10 wt% carbon (sucrose acts as carbon source). The mixture was pre-sintered in a tube furnace with the flowing Ar–H_2 (92:8, *v*/*v*) at 350 °C for 6 h. After cooling to room temperature, the samples were reground for 4 h, then calcined at different temperatures from 400 to 700 °C for 10 h and cooled down to room temperature in the tube furnace under the same atmosphere. Note that the sample prepared at 300 °C is referred to the one by direct calcining at 300 °C for 10 h without the pre-sintering process. To study the reaction mechanism, the mixture of NaF and $FeC_2O_4 \cdot 2H_2O$ (2:1 in mole) was calcined with the same procedure as the sample synthesized at 300 °C. Additionally, the Na_2FePO_4F/C sample prepared at 600 °C was re-sintered at 800 °C for 10 h under Ar and the tail gas was flown into the deionized water to identify whether fluorine element was released at high temperature.

The composite electrode was composed of active material, Super P and polyvinylidene fluoride (PVDF) at a weight ratio of 80:10:10. Slurries containing three components in N-methyl-pyrollidone (NMP) were prepared and casted on Al-foil current collectors. After drying at 120 °C under vacuum overnight, the electrodes were punched into Φ 16 mm disks with active material loading of about 3.48 mg/cm^2. The electrochemical performance was evaluated using 2032 coin cells. Metallic lithium was used as the counter electrode, 1 mol L^{-1} $LiPF_6$ was dissolved in ethylene carbonate (EC)/dimethyl carbonate (DMC) (1:1, *v*/*v*) as electrolyte, and glass fiber as separator. Test cells were assembled in an M-Braun glove box filled with pure argon.

The electrochemical measurements were carried out on a PC-controlled Land Battery Tester (Jinnuo, Wuhan). For the testing, we adopted the constant current–constant voltage (CC–CV) charging system: the cells were charged galvanostatically to 4.5 V at 0.1 C (1 C = 124 mAh g^{-1}), kept at 4.5 V until the current dropped to 0.02 C, and then discharged to 2.0 V at 0.1 C. During the rate performance measurements, the cells were charged to 4.5 V at the specific rate (0.05 C, 0.2 C, 0.5 C, 2 C and 0.05 C), kept at 4.5 V until the current dropped to 0.02 C and then discharged to 2.0 V at the same rate respectively. For every rate, five cycles were performed. To explore the possibility of extracting the second cation in Na_2FePO_4F, the cell based on as-prepared Na_2FePO_4F at 600 °C was charged to the higher potential (5.1 or 5.2 V). For this test, the cells were galvanostatically cycled with a current density of 0.1 C. The electrochemical capacity of the samples was calculated based on the amount of pure active materials excluding the coated carbon.

Crystal structures were characterized by X-ray diffraction (XRD) (D8 Advance, Bruker AXS, Germany) with Cu Kα radiation (40 KV, 40 mA). The sample for refinement was scanned from $2\theta = 10°$ to 130° with a rate of 1° per minute. The structural parameters were refined by the Rietveld analysis that was performed with the Jana2006 program (Windows version, 2011). Surface morphology was observed by scanning electron microscopy (S4800, Hitachi, Japan). The carbon content was verified by an organic element analyzer (PE2400II, USA). Thermal analysis was carried out on TG/DTA instrument (Pryis Diamond, Perkin-Elmer, USA) with a heating rate of 5 °C min^{-1} under N_2 flow between 30 and 800 °C. The content of F element in water was detected with the ion analyzer (PXSJ-216, Shanghai).

3. Results and discussion

XRD patterns of samples prepared at various temperatures were shown in Fig. 1a. The Na_2FePO_4F phase appeared in the as-prepared sample at 300 °C. Pure crystalline Na_2FePO_4F could be obtained at the calcined temperature between 400 and 600 °C, and its crystallization was improved as the synthetic temperature increased. When the calcined temperature further increased, Na_2FePO_4F started to decompose, and the decomposition products became the dominant phase in the sample synthesized at 800 °C. The presented species were attributed to Fe metal, Na_3PO_4 and $Fe_3(PO_4)_2$, as labeled in Fig. 1a. Therefore, the calcined temperature should be set under 650 °C. It should be noted that F element was not examined in the decomposition products.

To acquire the lattice parameters, the XRD pattern of Na_2FePO_4F prepared at 600 °C was re-collected with a slower scanning rate of 1° per minute, and was refined by the Rietveld analysis with Jana2006 program, as shown in Fig. 1b. It can be seen that no impurity peak was detected, indicating the high purity of Na_2FePO_4F was formed at 600 °C. Pure Na_2FePO_4F exhibited the orthorhombic structure indexed in the *Pbcn* space group. The lattice

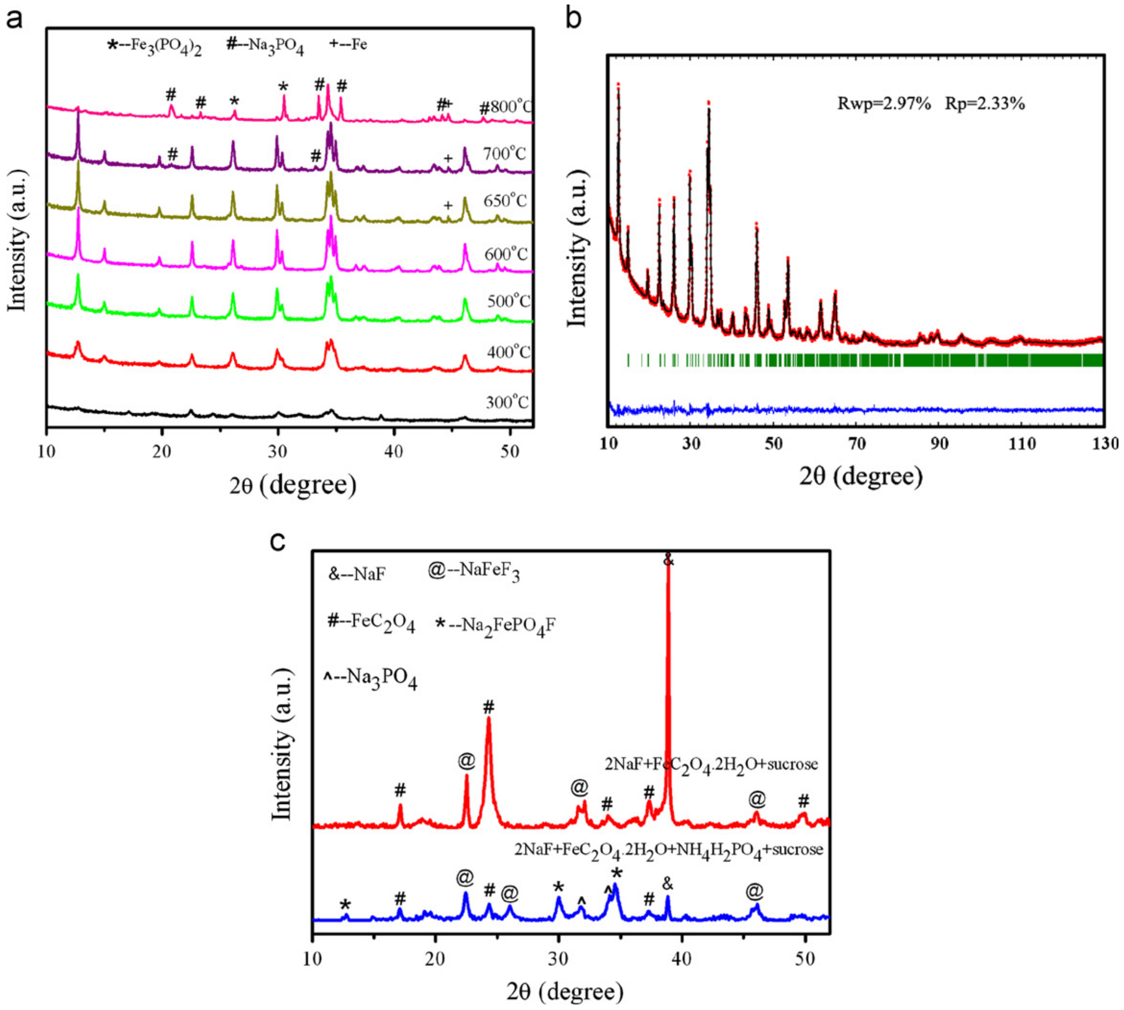

Fig. 1. (a) XRD patterns of Na_2FePO_4F/C samples prepared at various temperatures. (b) Full XRD pattern and Rietveld refinement result of Na_2FePO_4F/C prepared at 600 °C. (c) XRD patterns of the mixture of $NaF+FeC_2O_4\cdot 2H_2O$ (2:1 in mole)+sucrose and $NaF+FeC_2O_4\cdot 2H_2O+NH_4H_2PO_4$ (2:1:1 in mole)+sucrose prepared at 300 °C for 10 h.

parameters were $a=5.240855$ Å, $b=13.85140$ Å and $c=11.78998$ Å. These results were consistent with those reported in previous Refs. [5,7].

According to the XRD pattern of the sample prepared at 300 °C, $NaFeF_3$ (PDF#43-0705) could be identified as the interphase in the solid-state reaction, as shown in Fig. 1c. Namely, $NaFeF_3$ originated from the reaction of NaF and $FeC_2O_4\cdot 2H_2O$. To verify this assumption, a mixture of NaF and $FeC_2O_4\cdot 2H_2O$ (2:1 in mole) was directly calcined at 300 °C for 10 h. We found that its XRD pattern also contained the peaks corresponding to crystalline $NaFeF_3$ (see the upper pattern in Fig. 1c). Also, the intensity of FeC_2O_4 peak at 24.5° was much stronger than that in the sample at 300 °C. This revealed that, in the sample at 300 °C, H_3PO_4 (from the decomposition of $NH_4H_2PO_4$) reacted with FeC_2O_4 to produce an amorphous material, which was identified as $FeHPO_4$ according to the previous work [10]. On the other hand, Na_3PO_4, which should be the reaction product of NaF and H_3PO_4, was also detected in the sample at 300 °C.

Fig. 2 showed the TG/DTA curves of the precursor without sucrose. In the DTA curve, the only endothermic peak occurred at 180 °C, corresponding to the reaction of losing crystal water from $FeC_2O_4\cdot 2H_2O$ [12]. From room temperature to 430 °C, the weight loss was 40.7 wt%, which was close to the calculated value (43 wt%) according to the formation reaction of Na_2FePO_4F from precursors. This indicated that the reaction almost ended up at ~430 °C. At temperature ranging from 490 to 640 °C, the reaction was endothermic, although no weight loss was observed. Therefore, we can say that the improvement of crystallization was mainly involved in this range. When temperature exceeded 640 °C, the sample's weight loss restarted and reached 2.9 wt% at 800 °C. Since F element was not detected in the decomposition products in the XRD results (see Fig. 1a), this type of weight loss should be related to the releasing of F element from the Na_2FePO_4F lattice. Note that the releasing of F element should result a weight loss of 5.0 wt% in theory. To verify this assumption, the sample prepared at 600 °C was re-sintered

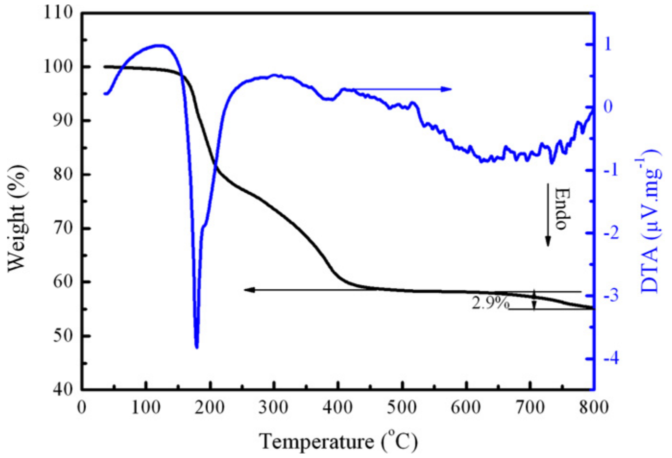

Fig. 2. TG/DTA curves of the precursors without sucrose in N_2 atmosphere. The scan rate is 5 °C min^{-1} from 30 to 800 °C.

at 800 °C for 10 h under Ar and the tail gas was flown into the container with the deionized water. Results indicated that F element was indeed detected in the deionized water, revealing that F element was released in the gaseous state. Moreover, this gas is more likely F_2 than HF under Ar atmosphere.

Based on the above results and analysis, we proposed that the whole process of the solid-state reaction could be divided into three main steps. The first step was the pre-reaction to form interphases. NaF was involved in the pre-reaction to form $NaFeF_3$ and Na_3PO_4 as the crystalline interphase materials. In contrast, the precursor LiF was kept intact in the case of synthesizing $LiFePO_4$ [10]. Amorphous $FeHPO_4$ was the other interphase material in this stage. The pre-reaction should proceed as shown in Eq. (1). The second step was the formation of Na_2FePO_4F phase (Eq. (2)). Na_2FePO_4F phase appeared at 300 °C and started to form the only crystalline phase at 400 °C. Its crystallization was continuously improved until 600 °C. Notably, the first and second steps were actually interwoven together, as shown in Fig. 1c. The third step was the decomposition of Na_2FePO_4F, which occurred at 650 °C and above, as shown in Eq. (3). The decomposition products comprised of solid-phase Fe, Na_3PO_4 and $Fe_3(PO_4)_2$ and F_2 in gaseous state. Note that the thermal stability of Na_2FePO_4F was much poorer than that of olivine $LiFePO_4$ [10] and Li_2CoPO_4F [13].

$$2FeC_2O_4 \cdot 2H_2O + 2NH_4H_2PO_4 + 4NaF \rightarrow NaFeF_3 + FeHPO_4 + Na_3PO_4 + 6H_2O\uparrow + 2CO_2\uparrow + 2CO\uparrow + 2NH_3\uparrow + HF\uparrow \quad (1)$$

$$NaFeF_3 + FeHPO_4 + Na_3PO_4 \rightarrow 2Na_2FePO_4F + HF\uparrow \quad (2)$$

$$6Na_2FePO_4F \rightarrow 3Fe + 4Na_3PO_4 + Fe_3(PO_4)_2 + 3F_2\uparrow \quad (3)$$

The reaction mechanism to form Na_2FePO_4F was different from that of Li_2CoPO_4F, in which $CoHPO_4$ forms first, then $LiCoPO_4$ between 400 and 700 °C, and finally Li_2CoPO_4F above 700 °C [13]. The differences between reaction mechanisms of Li_2CoPO_4F and Na_2FePO_4F should be closely related to the bond energies between Li–F (545.6 kJ mol^{-1}) and Na–F (492.8 kJ mol^{-1}) [14]. As compared with the case of Li_2CoPO_4F, the weaker Na–F bonds enabled the reaction between NaF and FeC_2O_4 at 300 °C.

The surface morphologies of the samples were observed with SEM. Fig. 3a–d shows that as calcined temperature increased between 400 and 650 °C, the particle grew slightly from ~50 nm to ~200 nm. As for the sample prepared at 700 °C (see Fig. 3e), some large particles ~1 μm were observed in various scanned regions. EDS analysis in Fig. 3f indicated that Fe element was the dominant component in these large particles, which was consistent with the XRD result that metal Fe particles peak was detected in the sample at 700 °C in Fig. 1a. Table 1 listed the carbon contents in samples measured with organic element analyzer. It was reasonable that carbon content reduced as the calcined temperature increased and due to the enhanced extent of carbonization.

The electrochemical performances of Na_2FePO_4F/C samples prepared at 400, 500, 600 and 650 °C were evaluated using coin cells between 2.0 and 4.5 V vs. Li/Li$^+$. Charge–discharge curves in Fig. 4 showed that Na_2FePO_4F/C at 600 °C exhibited a discharge capacity of 118 mAh g^{-1} between 2.0 and 4.5 V vs. Li/Li$^+$ at 0.05 C, close to the theoretical value of the one-electron reaction(124 mAh g^{-1}). The rate performances were shown in Fig. 5. It was found that, even at 0.5 C and 2 C, the sample synthesized at 600 °C showed a discharge capacity of 113 mAh g^{-1} and 106 mAh g^{-1}, respectively, corresponding to 95.8% and 89.8% of that at 0.05 C. Owing to the impurities and larger particle size, Na_2FePO_4F/C prepared at 650 °C exhibited a little lower discharge capacity and slightly poorer rate performance. It showed a discharge capacity of 111 mAh g^{-1} at 0.05 C, and remained 86.0% at 0.5 C and 70.2% at 2 C. The Na_2FePO_4F/C samples sintered at 500 and 400 °C showed much worse electrochemical performances. Their discharge capacities were 105 and 78 mAh g^{-1} at 0.05 C, respectively. The capacity retentions at 2 C were 55.2% and 14.1%, respectively. This can be explained by the poor crystallization of samples prepared below 600 °C, which was also observed in $LiFePO_4$ samples synthesized at low temperatures [15]. Therefore, the excellent electrochemical performance can be attributed to its good crystallization and high purity of Na_2FePO_4 formed at 600°C.

Fig. 6 compared the cyclic performances of Na_2FePO_4F/C samples prepared at 400, 500, 600 and 650 °C. The samples prepared at 600 and 650 °C showed good cyclic stabilities, and kept discharge capacities of 115 and 109 mAh g^{-1} at the 100th cycle respectively, corresponding to 97.5% and 98.2% of capacity retention. This indicated that Na_2FePO_4F/C samples at 600 and 650 °C showed structural stability to stand the long-term cycling. In contrast, the capacity fading of Na_2FePO_4F/C samples at 400 and 500 °C was much serious. The capacity losses were 12 and 13 mAh g^{-1} after 100 cycles, respectively. This bad cyclic stability was also due to the poor crystallization.

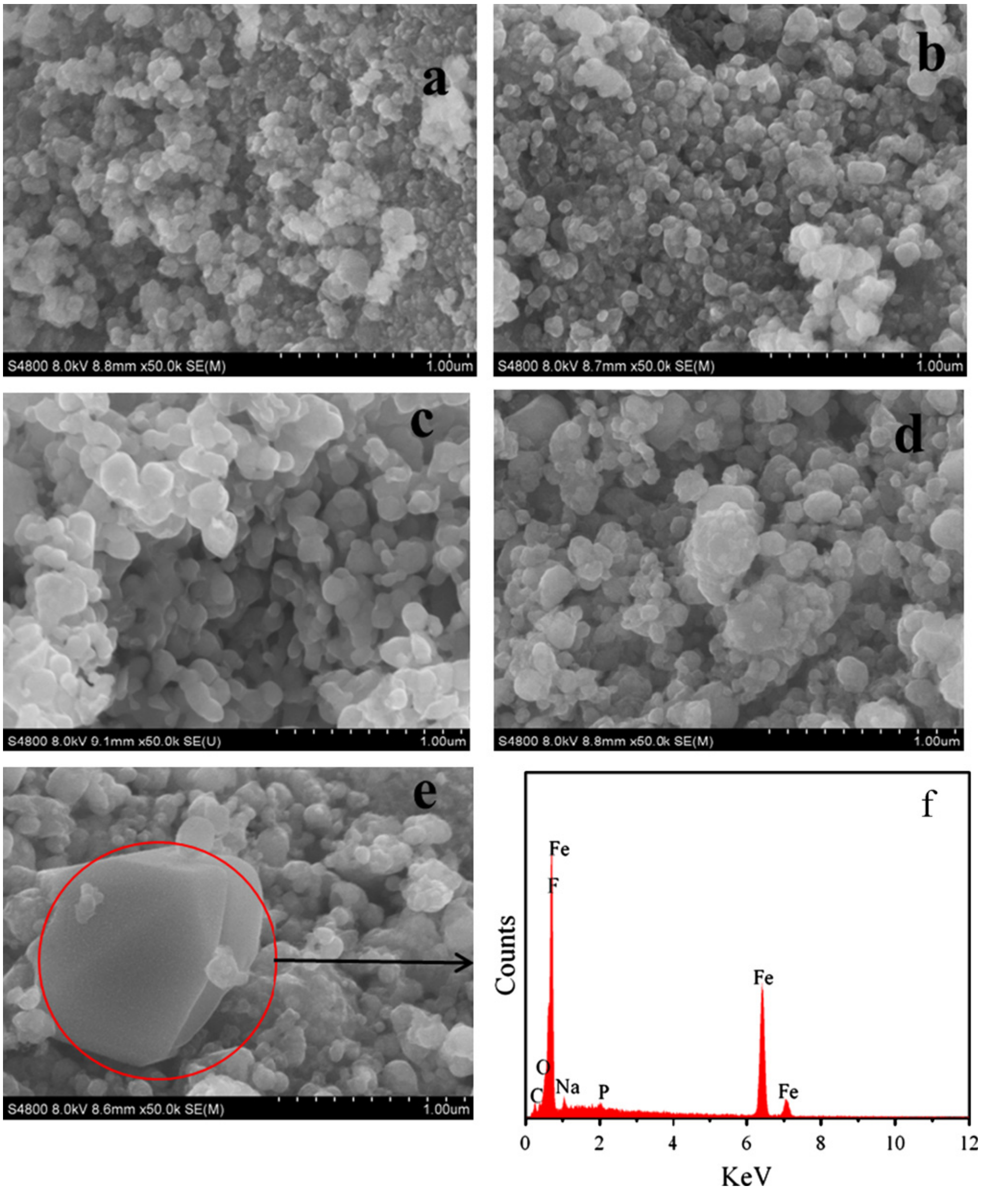

Fig. 3. SEM images of Na_2FePO_4F/C samples prepared at (a) 400 °C, (b) 500 °C, (c) 600 °C, (d) 650 °C, and (e) 700 °C. (f) EDS spectroscopy of the large particle in (e).

Table 1
Carbon contents of Na_2FePO_4F/C samples prepared at various temperatures.

Calcined temperature (°C)	400	500	600	650	700
Carbon content (wt%)	7.87	7.57	7.24	7.08	6.31

Since it exhibited the best electrochemical performance, Na_2FePO_4F/C prepared at 600 °C was utilized to explore the possibility of utilizing the second Na^+. Na_2FePO_4F/C was charged to the various potentials higher than 5 V vs. Li/Li^+, which were more than 500 mV, higher than those in other Refs. [1,5,8]. When the cell was cycled between 2.0 and 5.1 or 5.2 V vs. Li/Li^+, the discharge capacities were maintained at ~120 mAh g^{-1} in the first and second cycles, as shown in Fig. 7a and b. Also, the discharge curves almost overlapped than that measured between 2.0 and 4.5 V vs. Li/Li^+, indicating that the second Na^+ was not extracted up to 5.1 or 5.2 V. Note that the irreversible capacity loss of *ca.* 20 mAh g^{-1} is due to the electrolyte oxidative decomposition. When the sample was charged to 5.3 V or higher, the discharge performances of Na_2FePO_4F/C were significantly influenced by the electrolyte decomposition.

4. Conclusions

We demonstrated that the pure Na_2FePO_4F/C phase could be prepared with NaF as the only sodium precursor. The sample synthesized at 600 °C exhibited the best electrochemical performance due to the good crystallization and high phase purity. The second Na^+ could not be extracted even when Na_2FePO_4F/C was charged to 5.2 V vs.

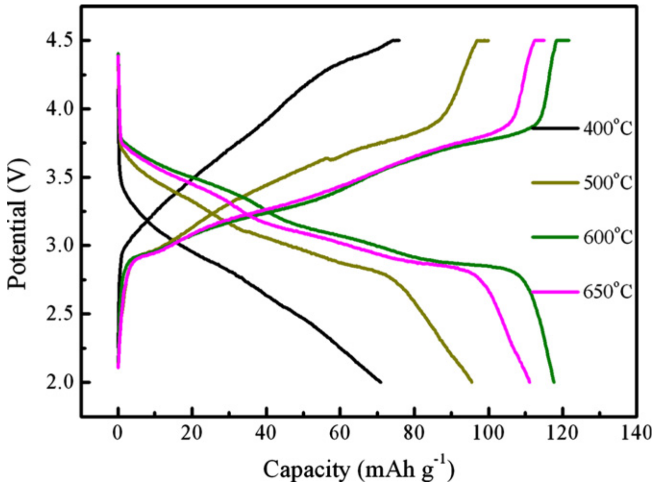

Fig. 4. Charge–discharge curves of second cycle of Na_2FePO_4F/C samples prepared at 400, 500, 600 and 650 °C. The rate was 0.05 C.

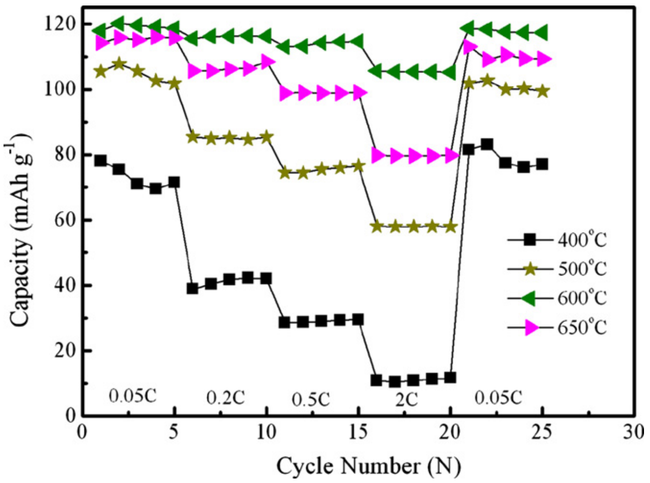

Fig. 5. Rate performances of Na_2FePO_4F/C samples prepared at 400, 500, 600 and 650 °C.

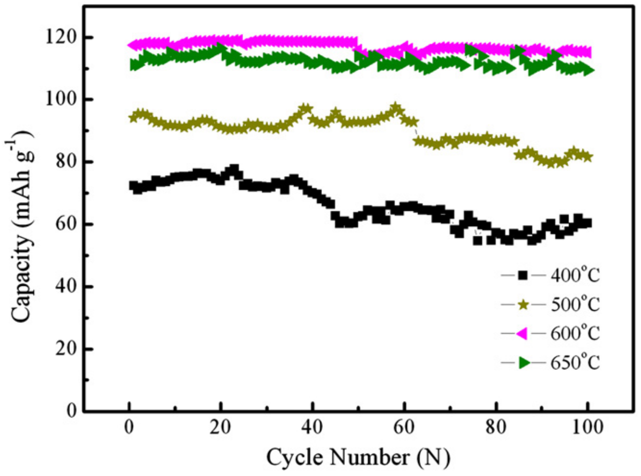

Fig. 6. Cyclic performances of Na_2FePO_4F/C samples prepared at 400, 500, 600 and 650 °C. The rate was 0.1 C.

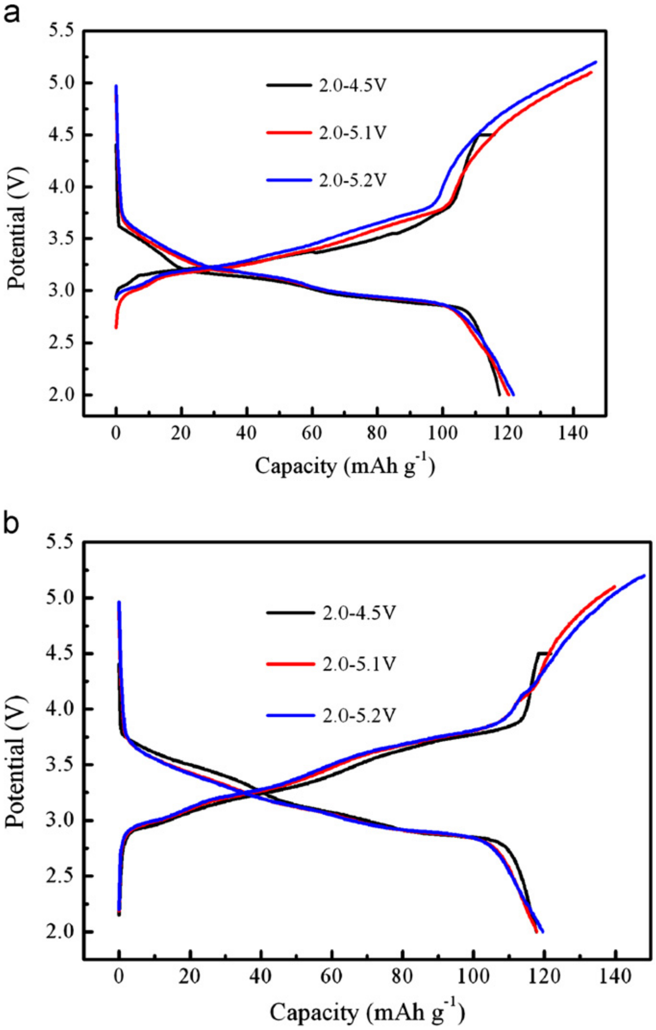

Fig. 7. Charge–discharge curves of (a) first and (b) second cycles of Na_2FePO_4F/C sample prepared at 600 °C with the cut-off potential of 4.5, 5.1 and 5.2 V vs. Li/Li^+. The rate was 0.1 C.

Li/Li^+, at which electrolyte obviously decomposed. Therefore, finding an electrolyte which is stable at higher potential has become a prerequisite to investigate the characteristics of extracting/inserting the second alkaline cation of A_2MPO_4F.

Acknowledgments

The authors thank Ningbo Key Innovation Team (No. 2011B82005), 973 Project (No. 2012CB722704), 100 Talents Program, Chinese Academy of Science (NIMTE, CAS) and National Natural Science Foundation of China (NSFC) (No. 51072183) for financial supports.

References

[1] B.L. Ellis, W.R.M. Makahnouk, Y. Makimura, K. Toghill, L.F. Nazar, A multifunctional 3.5 V iron-based phosphate cathode for rechargeable batteries, Nature Materials 6 (2007) 749–753.

[2] N. Recham, J.N. Chotard, L. Dupont, K. Djellab, M. Armand, J.M. Tarascon, Ionothermal synthesis of sodium-based

fluorophosphate cathode materials, Journal of the Electrochemical Society 156 (12) (2009) A993–A999.

[3] M. Ramzan, S. Lebègue, R. Ahuja, Ab initio study of lithium and sodium iron fluorophosphate cathodes for rechargeable batteries, Applied Physics Letters 94 (2009) 1519041–1519043.

[4] M. Ramzan, S. Lebègue, P. Larsson, R. Ahuja, Structure, magnetic, and energetic properties of Na_2FePO_4F, Li_2FePO_4F, $NaFePO_4F$, and $LiFePO_4F$ from *ab initio* calculations, Journal of Applied Physics 106 (2009) 0435101–0435106.

[5] B.L. Ellis, W.R.M. Makahnouk, W.N.R. Weetaluktuk, D.H. Ryan, L.F. Nazar, Crystal structure and electrochemical properties of A_2MPO_4F fluorophosphates (A = Na, Li; M = Fe, Mn, Co, Ni), Chemistry of Materials 22 (2010) 1059–1070.

[6] Y. Kawabe, N. Yabuuchi, M. Kajiyama, N. Fukuhara, T. Inamasu, R. Okuyama, I. Nakai, S. Komaba, Synthesis and electrode performance of carbon coated Na_2FePO_4F for rechargeable Na batteries, Electrochemistry Communications 13 (2011) 1225–1228.

[7] I.K. Lee, I.B. Shim, C.S. Kim, Phase transition studies of sodium deintercalated $Na_{2-x}FePO_4F$ ($0 \leq x \leq 1$) by Mössbauer spectroscopy, Journal of Applied Physics 109 (2011) 07E1361–07E1363.

[8] X.B. Wu, J.M. Zheng, Z.L. Gong, Y. Yong, Sol–gel synthesis and electrochemical properties of fluorophosphates $Na_2Fe_{1-x}Mn_xPO_4F/C$ ($x = 0$, 0.1, 0.3, 0.7, 1) composite as cathode materials for lithium ion battery, Journal of Materials Chemistry 21 (2011) 18630–18637.

[9] Y. Kawabe, N. Yabuuchi, M. Kajiyama, N. Fukuhara, T. Inamasu, R. Okuyama, I. Nakai, S. Komaba, A comparison of crystal structures and electrode performance between Na_2FePO_4F and $Na_2Fe_{0.5}Mn_{0.5}PO_4F$ synthesized by solid-state method for rechargeable Na-ion batteries, Electrochemistry 80 (2) (2012) 80–84.

[10] D.Y. Wang, H. Li, Z.X. Wang, X.D. Wu, Y.C. Sun, X.J. Huang, L.Q. Chen, New solid-state synthesis routine and mechanism for $LiFePO_4$ using LiF as lithium precursor, Journal of Solid State Chemistry 177 (2004) 4582–4587.

[11] P. Fu, Y.M. Zhao, Y.Z. Dong, X.N. An, G.P. Shen, Low temperature solid-state synthesis routine and mechanism for $Li_3V_2(PO_4)_3$ using LiF as lithium precursor, Electrochimica Acta 52 (2006) 1003–1008.

[12] L.N. Wang, Q.X. Sun, K.L. Zhang, Kinetics of thermal decomposition of $FeC_2O_4 \cdot 2H_2O$ in air, Journal of Wuhan University (Natural Science Edition) 53 (6) (2007) 635–640.

[13] D.Y. Wang, J. Xiao, W. Xu, Z.M. Nie, C.M. Wang, G. Graff, J.G. Zhang, Preparation and electrochemical investigation of Li_2CoPO_4F cathode material for lithium-ion batteries, Journal of Power Sources 196 (2011) 2241–2245.

[14] J. Zhang, X.Z. Duan, The relation between atomic potentials and dissociation energy of chemical bonds, Journal of Xinyang Teachers College (Nature Science Edition) 5 (4) (1992) 421–426.

[15] A. Yamada, S.C. Chung, K. Hinokuma, Optimized $LiFePO_4$ for lithium battery cathodes, Journal of the Electrochemical Society 148 (3) (2001) A224–A229.